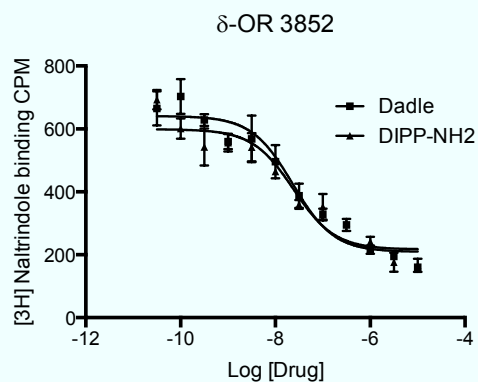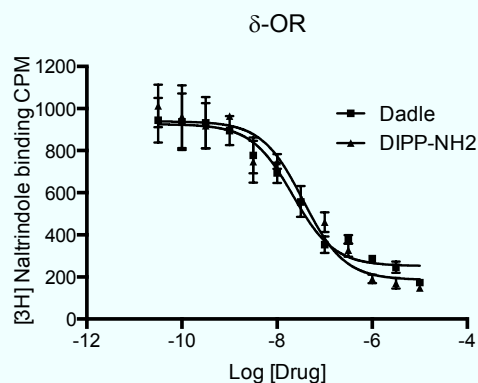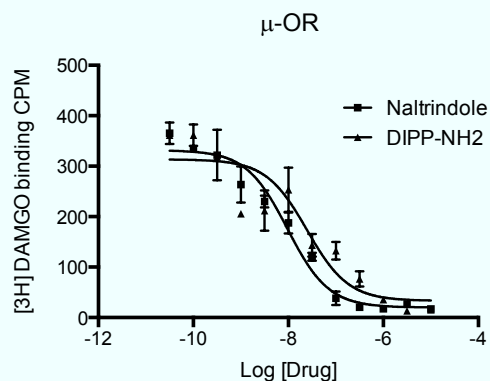**Supplementary Figure 1**

**Crystals of BRIL$_{\Delta38}$δ-OR–-DIPP-NH$_2$ used for Synchrotron and XFEL data collection.**

a, Brightfield and **b,** cross-polarized images of BRIL$_{\Delta38}$δ-OR–DIPP-NH$_2$ crystals used to obtain the synchrotron structure. **c,** Brightfield and **d**, cross-polarized images of BRIL$_{\Delta38}$δ-OR–DIPP-NH$_2$ microcrystals after optimization of crystal growth conditions to yield crystals of ~5 µm, suitable for LCP crystallization in syringes. **e,f,** Cross-polarized images of BRIL$_{\Delta38}$δ-OR–DIPP-NH$_2$ LCP microcrystals grown in syringes and used to obtain the XFEL BRIL$_{\Delta38}$δ-OR–DIPP-NH$_2$ structure.

μ-OR

	Naltrindole	DIPP-NH2
Ki	4.789e-009	1.240e-008

δ-OR

	Dadle	DIPP-NH2
Ki	1.069e-008	1.779e-008

δ-OR 3852

	Dadle	DIPP-NH2
Ki	1.161e-008	1.209e-008

Supplementary Figure 2

Radioligand binding data for small molecule and peptide to μ-OR and δ-OR.

Binding data of DIPP-NH$_2$ and naltrindole to WT μ-OR, and of DIPP-NH$_2$ and DADLE to both WT δ-OR and BRIL$_{\Delta 38}$δ-OR using the peptide [^{3}H]DAMGO and small molecule [^{3}H]naltrindole as competing radioligands. Results represent mean ± SEM of three independent experiments each in quadruplicate.
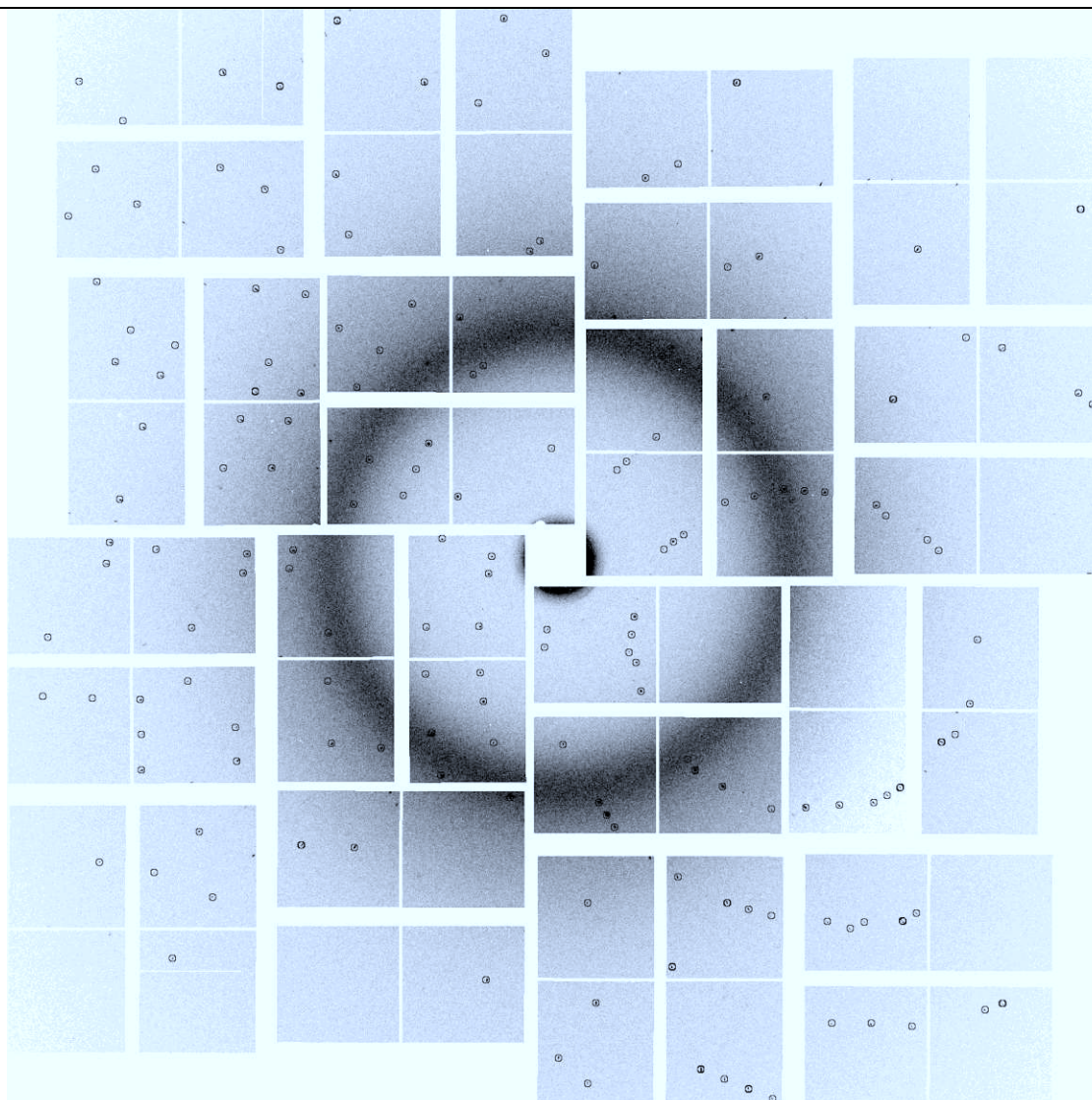
Supplementary Figure 3

XFEL single diffraction image.

Diffraction pattern from a $BRIL_{\Delta 38}\delta$-OR–DIPP-NH_2 microcrystal in LCP. Diffraction peaks identified by Cheetah program are circled. The edge of the detector corresponds to a resolution of 2.1 Å.
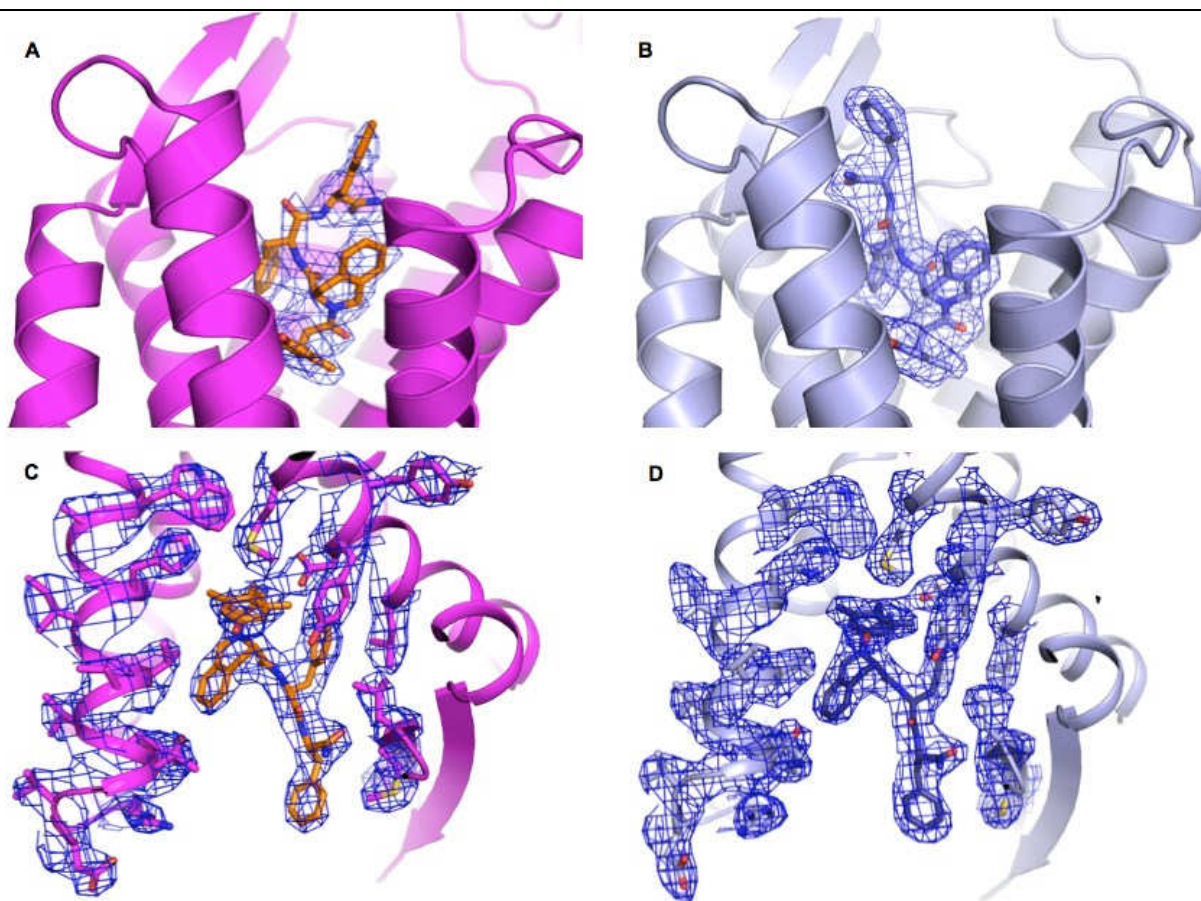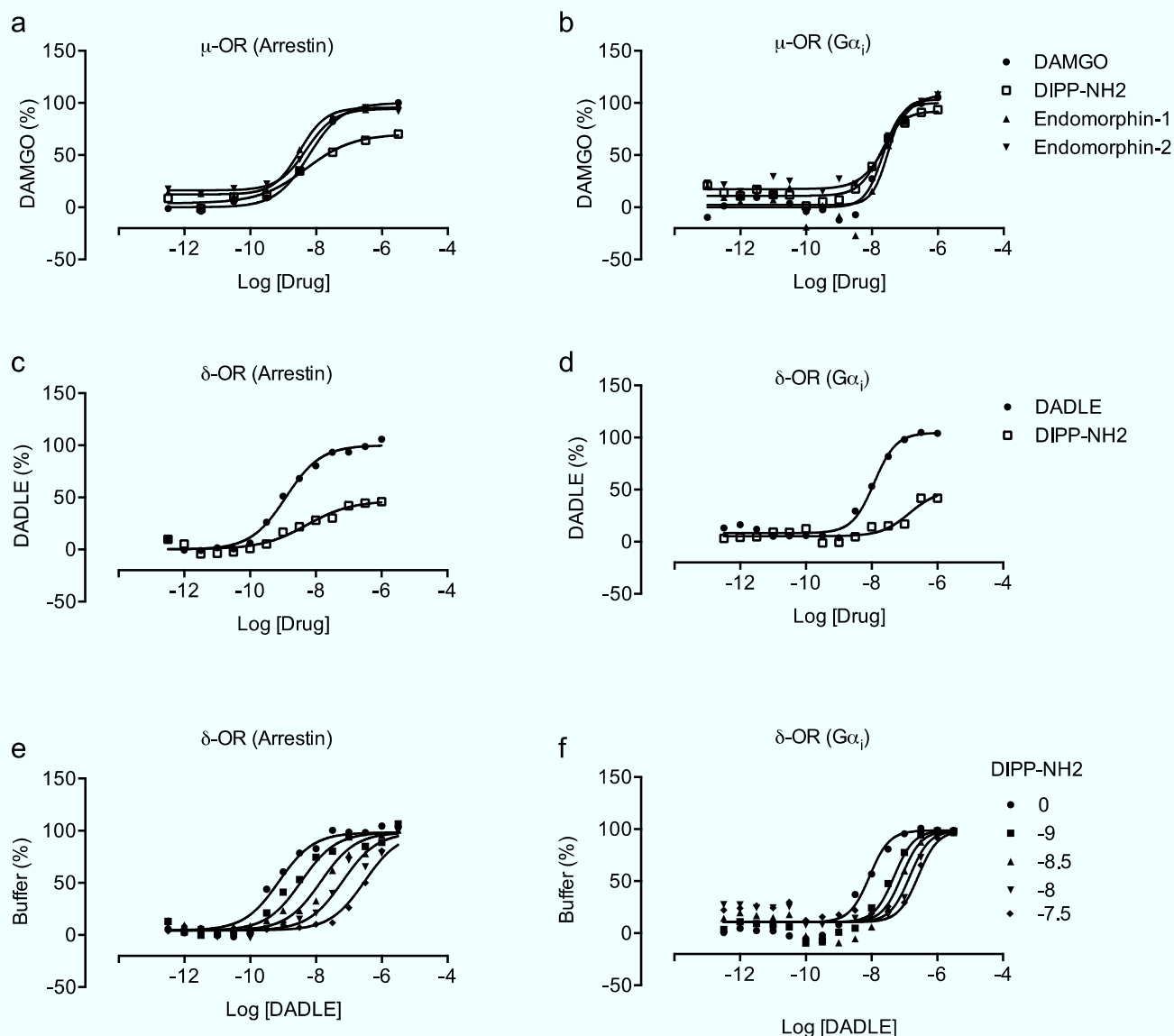
Supplementary Figure 4

Electron density around the peptide-binding site in the Synchrotron and XFEL structures.

a and **b**, Two different binding conformations for Phe(4)-NH$_2$ residue of the tetrapeptide DIPP-NH$_2$ are found in molecule B of the Synchrotron (**a**) and XFEL (**b**) structures. The 2Fo-Fc electron density contoured at 1σ (blue mesh) is shown around the ligand.
c and **d**, DIPP-NH2 adopts the same binding mode in molecule A of the synchrotron (**c**) and XFEL structures (**d**). Synchrotron structure is shown as magenta cartoon with DIPP-NH$_2$ as orange sticks, and XFEL structure is shown as light blue cartoon with DIPP-NH$_2$ as blue sticks. A comparison between the quality of the electron density between Synchrotron and XFEL structures are shown in (**c**) and (**d**).

Supplementary Figure 5

Functional characterization of peptide ligands at the human μ-OR and δ-OR.

Efficacy and potency of the bi-functional ligand DIPP-NH2, the synthetic peptide ligand DAMGO as well as the endogenous opioid peptide endomorphin-1 and -2 were characterized at the μ-OR for arrestin recruitment using a BRET-based bioassay (**a**) and at the $G\alpha_i$-protein pathway using a Glosensor-based bioassay (**b**). Results are reported as normalized concentration-responses induced by the selective μ-OR peptide ligand DAMGO. Similarly, the pharmacological profile of DIPP-NH₂ toward the δ-OR was measured using a tango-based assay for arrestin recruitment (**c,e**) and Glosensor for $G\alpha_i$ activation (**d,f**). Normalized dose-response induced by the δ-OR peptide ligand DADLE is reported. **e,f**, Schild regression analysis at δ-OR arrestin recruitment and $G\alpha_i$ activity was performed with various concentration of DIPP-NH₂ over a DADLE dose-response curve. Results represent mean ± SEM of three independent experiments each in quadruplicate.